Cell, Volume *133*

Supplemental Data

Meiotic Chromosomes Move by Linkage to Dynamic Actin Cables with Transduction of Force through the Nuclear Envelope

R. Koszul, K.P. Kim, M. Prentiss, N. Kleckner, and S. Kameoka

Note S1

All images were analyzed using ImageJ (Abramoff et al. 2004) and/or Metamorph™ functions. Deconvolution of 2D and 3D acquisitions was performed using AutoDeblur®.

Persistence length calculation

Persistence length (Lp) of *in vitro* chromosomes was determined from individuals free in solution or attached by one end to a chromosomal clump as visualized by DAPI-staining, which shows a much more stable signal than Zip1-GFP. *In vivo*, it is much easier to distinguish Zip1-GFP chromosomes from one another than with DAPI-stained chromosomes; thus, *in vivo* persistence length was calculated from Zip1-GFP images (strain NKY3834). Lp was determined as described (Ott et al., 1993; Houchmandzadeh and Dimitrov, 1999). A frame from a Zip1-GFP movie, containing clearly individualized chromosomes, is selected (Figure S1Ai, ii). The axis of a chromosome lying within the focal plane was outlined by choosing the brightest center pixels (iii). From one end of the axis, a circle of 0.8μm radius was drawn (iv). At the interaction of this first circle with the axis, a second similar circle was drawn (v). The three points where the axes cross a circle line are successively rejoined to form segments, or tangent vectors (vi, vii). Ideally, several tangent vectors would be drawn along a unique axis (Ott et al., 1993). However, due to the short size of our material (longest chromosomes are ~1.6 – 2μm in size) we cannot draw more than two such vectors. We used an arc length of 0.8μm, which corresponds to ~12 pixels. The suitability of this length was determined by trial and errors assays. This length permits us to study long chromosomes at our current resolution with fair confidence. Theory predicts that for an ideal polymer, the mean dot product between two tangent vectors **t**(i) is linked to the persistence length by the equation: $\langle \mathbf{t}(s).\mathbf{t}(s+x) \rangle = \exp(-x/Lp)$ where x is the distance from the original position s (Houchmandzadeh and Dimitrov, 1999). In our case, and for the reasons explained

above, s always corresponds to the center of the first circle, and x = 0.8μm.

Supplemental References

Abramoff, M., Magelhaes, P., and Ram, S. (2004). Image processing with Image J. Biophotonics Int. *11*, 36-42.

Houchmandzadeh B. and Dimitrov S. (1999). Elasticity measurements show the existence of thin rigid cores inside mitotic chromosomes. J Cell Biol. *145*, :215-223.

Ott A, Magnasco M., Simon A., and Libchaber A. (1993). Measurement of the persistence length of polymerized actin using fluorescence microscopy. Phys Rev E Stat Phys Plasmas Fluids Relat Interdiscip Topics. *48*, R1642-R1645.

Note S2

What determines differential chromosome disposition at zygotene and pachytene?

Movements of chromosomes at the zygotene and pachytene stages present flagrant similarities. But the major difference between zygotene and pachytene appears to be whether localization and movement involves a single individual chromosome end, as at pachytene, or multiple co-localized (and sometimes, but not always, directly clustered) chromosome ends at zygotene. What could account for such a change?

In light of the findings, what determines the difference in overall patterns of chromosome disposition at zygotene and pachytene? And why/how does the situation change during the transition between the two stages? We propose that the only difference is the state of the chromosomes which, in diverse organisms, are longer, thinner and more flexible at zygotene and shorter, fatter and stiffer at pachytene. The zygotene chromosome state would permit clustering of multiple telomeres in a confined region of the NE (as well as, and presumably facilitated by, direct telomere-telomere aggregation). The pachytene chromosome state, in contrast, would preclude such colocalizations, effectively forcing an even distribution of chromosomes within the nucleus and thus an even distribution of their ends around the nuclear periphery. Images of DAPI-stained pachytene chromosomes strongly support the idea that chromosome state at this stage is incompatible with telomere clustering (e.g. Figure 4).

This formulation can also explain the fact that telomere movement during zygotene does not involve the strong outward-directed protrusions characteristic of

pachytene, as seen from analysis of both telomeres (Trelles-Sticken et al., 2005) and the NE (this work; Figure 3). Pachytene chromosomes are well-individualized discrete units that can be extracted out of the imbricated chromosomal set, resulting in chromosomal protrusions. Zygotene chromosomes, in contrast, are less well individualized and still in the process of achieving regular continuous juxtaposition of homologs and should therefore resist such extrication.

The stiffness of pachytene chromosomes could be determined by the state of the chromatin, rather than the mechanical properties of the SC (see results & discussion). By implication, variations in chromatin state between zygotene and pachytene could account for differences in global chromosome disposition at the two stages. In accord with this view:

- Chromatin at zygotene is highly compact while, at pachytene, chromatin is more expanded, as a general feature of meiosis in many organisms (e.g. Kleckner et al., 2004) including yeast (Figure S4AB). Since the chromatin fiber in an expanded condition is stiffer than that in a more compact condition, chromatin expansion should increase the stiffness of pachytene chromosomes as compared to their zygotene counterparts.

- A prediction of this relationship is that chromosomes with more compact chromatin will be "floppier" while chromosomes with more expanded chromatin will be "stiffer". In accord with this prediction, Sordaria chromosome axes are floppy at late zygotene and straight at mid-pachytene, implying more and less bending at the appropriate stages (Figure S4C). Even more strikingly (Figure S4B), spread yeast chromosomes at late zygotene, i.e. with essentially full length SCs but with their ends still in a bouquet, exhibit compact chromatin and have "floppy" SCs; moreover, chromosomes tend to lie one atop the other, another indication that "chromatin pushing" is absent. In contrast, pachytene chromosomes from the same preparations, which also have full length SCs, exhibit expanded chromatin and have "straight" SCs; moreover, chromosomes now lie side-by-side with each in its own territory, implying that chromatin pushing is present (Kleckner et al., 2004). These images support a determining role for chromatin expansion in the physical state of chromosomes during the progression from zygotene to pachytene.

Supplemental References

Kleckner, N., Zickler,, D., Jones, G.H., Dekker, J., Padmore, R., Henle, J., and Hutchinson, J. (2004). A mechanical basis for chromosome function. Proc. Natl. Acad. Sci. USA *101*, 12592-12597.

Trelles-Sticken, E., Adelfalk, C., Loidl, J., and Scherthan, H. (2005). Meiotic telomere clustering requires actin for its formation and cohesin for its resolution. J. Cell Biol. *170*, 213-223.

Note S3

Strains

General information

In NK3889, the *NDT80* gene is under the control of a chimeric transcription factor, Gal4-ER, which activates transcription only in the presence of β-estradiol in the medium (derived from strain KBY375, Benjamin et al. (2003)).

Abp140-GFP is derived from YCT791 (Taxis et al. 2006).

For Zip1-GFP, the GFP tag was inserted between AA700 and AA701 (Zip1-GFP(700)).

Nup49-GFP (Heun et al., 2001) and SPC42-YFP (details available upon request), tags are added to the C-terminus of the protein, with corresponding fusion genes present in their normal chromosomal contexts.

None of these fusion constructs impairs nor delays meiosis (e.g. Figure 5A).

Construction of the LatA/B-resistant (act1-117) SK1 strain

The original strain DDY0345 (*act1-117*::*HIS3*) is a gift from David Drubin (Wertman KF *et al.*, 1992). Genomic DNA was isolated and the DNA fragment containing *act1-117-HIS3* was amplified by PCR using primer *ACT1*-F1 (*TTTTTCTTCCCAAGATCGAAA*), and *ACT1*-R1 (*AACGCCGGACTCAAATTCTA*). The PCR fragment was gel-purified and transformed into haploid SK1 strain using *HIS3* marker, and integration was confirmed by PCR primers flanking integration junction regions. LatB-resistance was confirmed by growth on YPD plate supplemented with LatB (30 M), and the absence of wild type *ACT1* was confirmed by allele-specific PCR using primers ACT-117-F1 (*CGATTTGGCCGGTAGAGAT*) and ACT1-R3 (*TTTTGCATTCTTTCGGCAAT*).

Diploid strain with both *ZIP1-GFP* and *act1-117* was constructed by mating, resulting

SEY1082 (*ho::hisG/", LEU2/leu2, URA3/ura3, ZIP1::ZIP1-GFP(700)/", act1::act1-117-HIS3/"*).

Insertion of LacO arrays in yeast chromosomes

The *LacO* array derives from plasmid pLAU43 (gift from David Sherratt, Lau et al., 2003), which contains 240 copies of a non-repeat *LacO* operators and a kanamycin resistance marker is a gift from David Sherratt (Lau et al., 2003). The *Nhe*I-*Xba*I fragment of pLAU43 was subcloned into the *Sma*I site of pRS306 (*URA3* marker). The resulting plasmid pOL514 showed high transformation efficiency and good stability of the integrated LacO array.

(i) *LacO* array within the arm of Chromosome XV.

The *LacO* array was placed at the *TMA16* locus located 290kb and 480kb away from the telomere and centromere of Chromosome XV, respectively. A PCR amplification of the region was performed on SK1 genomic DNA (primers TMA16-F*TCAGGGCTACTATGCGTGAA* and TMA16-R *TGCCAATTTGTTTGTTACGG*). The resulting 600 bp fragment was subcloned into the *Eco*RI site of pOL514 to generate pOL519. pOL519 was digested with HpaI then transformed in a haploid *ura3* strain, and integrated transformants were selected by complementation on synthetic medium lacking uracile. Integration at *TMA16* locus was confirmed by PCR. Diploid strain NKY3840 (*ho/", ura3/URA3*::*CYC1p-LacI-GFP*, *leu2/", TMA16/TMA16*::*LacO-URA3*) was obtained through mating with a haploid strain expressing the *LacI*-GFP gene.

(ii) *LacO* array in chromosome XV telomeric position

The plasmid pJF83 containing 256 LacO array with telomere target (SCP1 locus) at one end of the chromosome XV was a gift of Shirleen Roeder (Fung et al, 2004)**.**

Construction of csm4Δ and ndj1Δ strains

Complete deletions of the *CSM4* and *NDJ1* genes were obtained by transformation of the SK1 strain YKK010 using a PCR-based protocol (Goldstein and McCusker, 1999). The *csm4Δ* and *ndj1Δ* mutations were marked with the *hphMX4* and *NatMX4* cassettes conferring resistance to hygromycin B and clonNat (nourseothricin), respectively (Goldstein and McCusker, 1999). *CSM4* deletion primers: RK-*CSM4hphf*-31 5'-*TTCTTCCCAAAAGGCAATATTGCAGAAGAAGAACTAGAAAatgCGTACGCTGCAGGTCGAC*-3' and RK-*CSM4hphr*-30 5'-GTATTTTTTTTATAGTAATAAATGCGAAATCATTAGCCACTTATTGAAAGTttaATCGAT

GAATTCGAGCTCG-3’ ; NDJ1 deletion primers: RK-*NDJ1natf*-64 5’-*GCAAAGAAAAGTTTTTTTTGGTTCAGATGTAATATGGATAGCCCGTTttaCGTACGCTGCAGGTCGAC*-3’ and RK-*NDJ1natr*-65
5’-
CTATACCATATACAACTTAGGATAAAAATACAGGTAGAAAAACTATAatgATCGATGAATTCGAGCTCG-3’. All constructions were verified by PCR and Southern blot analysis.

Construction of ZIP1-GFP(700)

ZIP1-GFP(700) was created by following the same method described in Whites *et al.* (2004) except that the GFP tag was inserted between AA700 and AA701 without stop codon, instead of AA525 and AA526, as suggested by D. Kaback and Z. Cande (personal communication; Scherthan et al., 2007). The GFP tag is flanked by peptide linkers GAPGG and
GSGCGRP in its N- and C-terminal positions, respectively.
Three PCR products ZIP1-AB, ZIP1-CD, and GFP were constructed, ligated together and subcloned into the *Kpn*I-*Not*I site of pEJW1 to replace ZIP1-GFP(525) with ZIP1-GFP (700), resulting in pOL526.
ZIP1-AB: A 2.9kb PCR fragment, carrying the promoter and N-terminal sequences of the *ZIP1* gene was amplified from pOL183 using primers A 5'-*GCTAGGTACCTATACAACCGATCGACAAATTAT*-3' and
B, 5'-*AAGCATGGCGCGCCTGTTATATCTTGCTTCTCCGAT*-3'. *Kpn*I and *Asc*I sites (underlined) were introduced at the 5' and 3' ends, respectively.
GFP: A 0.7kb PCR fragment corresponding to the GFP was gene amplified from pEJW1 (gift from Eric White (White *et al.*, 2004)) using primers 5'-*AAGCATGGCGCGCCTGGAGGTATGGCTAGCAAAGGAGAA*-3' and 5'-*AAGCATGGCCGGCCGCAGCCGGATCCTTTGTAT*-3'. *Asc*I and *Fse*I sites (underlined) were introduced at the 5' and 3' ends, respectively.
ZIP-CD: A 0.7 kb PCR fragment carrying the C-terminal and 3' region (UTR) of the *ZIP1* gene was amplified from pEJW1 using primer C, 5'-AGATGAGGCCGGCCAGCTGAAAAGTTAGAACTTCAAGATA -3' and primer D, 5'-ATGCTAGCGGCCGCGACCTCTTTTGTTTTTACTAGAG-3'. *Fse*I and *Not*I restriction sites (underlined) were introduced in the 3'-UTR to facilitate ligation into pRS plasmids.

Supplemental References

Fung, J.C., Rockmill B., Odell M., and Roeder, G.S. (2004). Imposition of crossover interference through the nonrandom distribution of synapsis initiation complexes. Cell. *116*, 795-802.

Goldstein A.L. and McCusker J.H. (1999). Three new dominant drug resistance cassettes for gene disruption in *Saccharomyces cerevisiae*. Yeast *15*, 1541–1553.

Lau I.F., Filipe, S.R., Soballe, B., Okstad, O.A., Barre, F.X., and Sherratt, D.J. (2003). Spatial and temporal organization of replicating *Escherichia coli* chromosomes. Mol. Microbiol. *49*, 731-743.

Scherthan, H., Wang, H., Adelfalk, C., White, E.J., Cowan, C., Cande, W.Z., and Kaback, D.B. (2007) Chromosome mobility during meiotic prophase in Saccharomyces cerevisiae. Proc Natl Acad Sci U S A. *104*, 16934-9.

Wertman, K.F., Drubin, D.G., Botstein, D. (1992). Systematic mutational analysis of the yeast *ACT1* gene. Genetics *132*, 337-350.

White, E.J., Cowan, C., Cande, W.Z., and Kaback, D.B. (2004). *In vivo* analysis of synaptonemal complex formation during yeast meiosis. Genetics. *167*, 51-63.

Benjamin, K.R., Zhang, C., Shokat, K.M., and Herskowitz, I. (2003). Control of landmark events in meiosis by the CDK Cdc28 and the meiosis-specific kinase Ime2. Genes Dev. *17*, 1524-1539.

Figure S1. (A) Persistence length calculation, described in Note S1. (B) Effect of LatB on the motion of Zip1-GFP labeled pachytene chromosomes (n=100 for each condition). Step size distribution of their centroids displacements recorded at 1 sec intervals. (top) chromosomes from a WT strain, with (magenta) or without (red) LatB. (bottom) chromosomes from a strain carrying the *act1-117* mutation that confer LatA/LatB resistance, in the presence (magenta) or absence (red) of LatB. (C) Rapid shift of a DAPI-labeled chromosomal mass. Movie recorded at 1 sec intervals. The corresponding displacement of the nucleus centroid is schematized on the right ([0 – 29] sec). Scale bar = 2 µm.

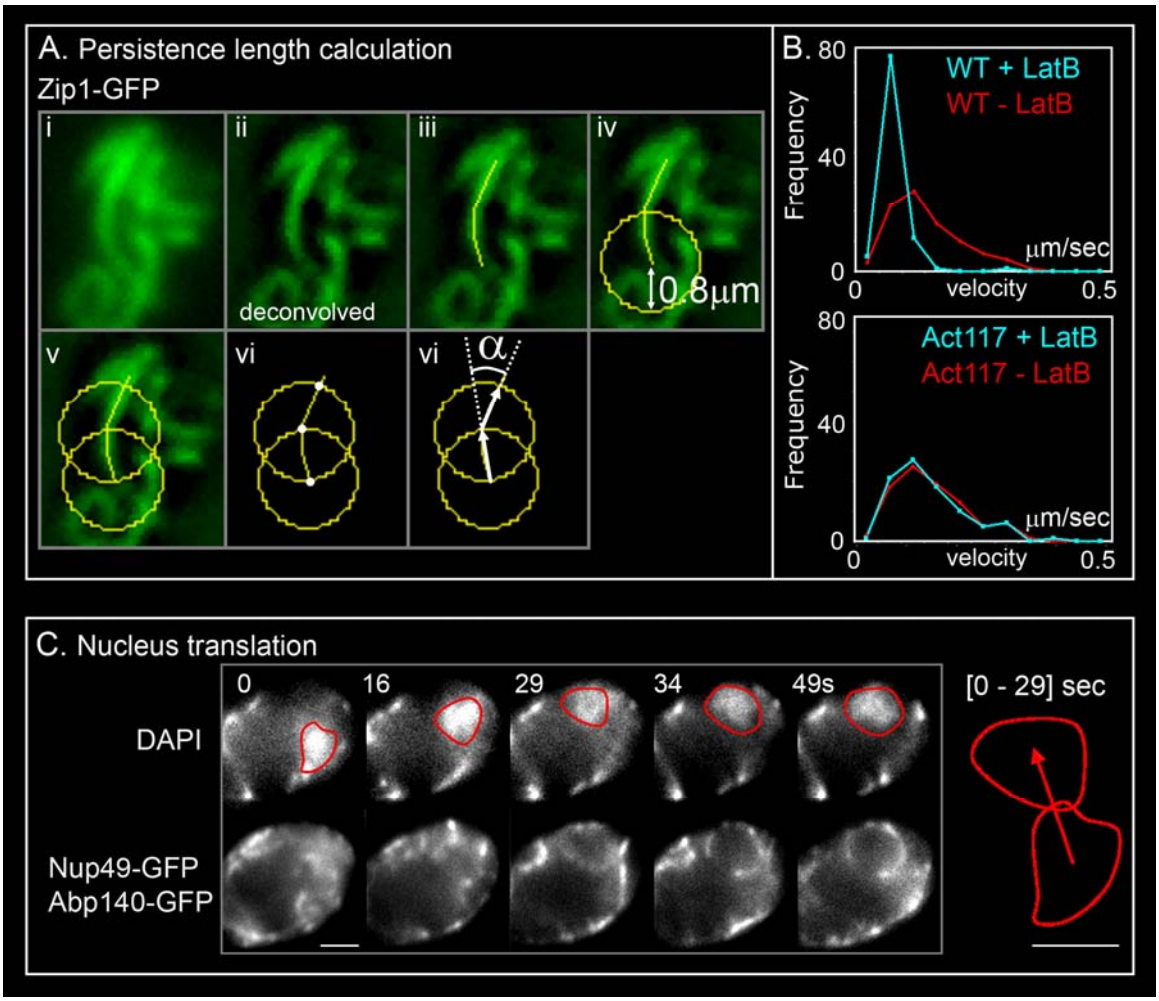

Figure S2. Persistence length calculation For every frame of Movie S3, Zip1-GFP chromosomes were outlined and binarization was performed so that the global nucleus shape deformation is now revealed by the white signal. For a given transition, a leader chromosome usually points out to a position in space designed as a focal point (see text and also Figure 2Aiii-vii). Here the focal points of consecutive transitions were defined for a single nucleus over several minutes and indicated with colored circles over the corresponding frames. Focal points occurring at a recurrent position were indicated using a same color. The last panel shows the summary of all the focal points defined over the time monitored.

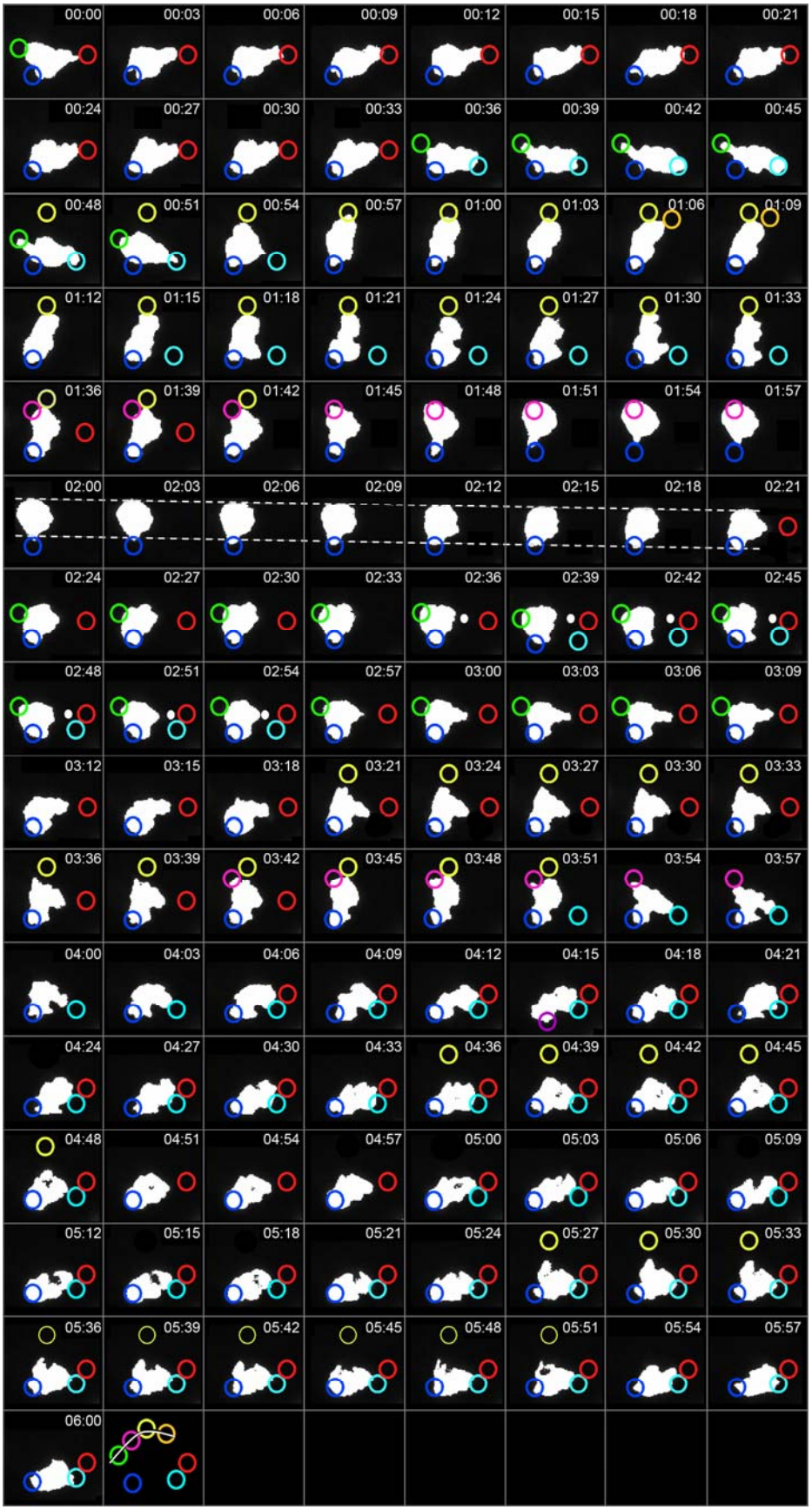
00:00
00:03
00:06
00:09
00:12
00:15
00:18
00:21
00:24
00:27
00:30
00:33
00:36
00:39
00:42
00:45
00:48
00:51
00:54
00:57
01:00
01:03
01:06
01:09
01:12
01:15
01:18
01:21
01:24
01:27
01:30
01:33
01:36
01:39
01:42
01:45
01:48
01:51
01:54
01:57
02:00
02:03
02:06
02:09
02:12
02:15
02:18
02:21
02:24
02:27
02:30
02:33
02:36
02:39
02:42
02:45
02:48
02:51
02:54
02:57
03:00
03:03
03:06
03:09
03:12
03:15
03:18
03:21
03:24
03:27
03:30
03:33
03:36
03:39
03:42
03:45
03:48
03:51
03:54
03:57
04:00
04:03
04:06
04:09
04:12
04:15
04:18
04:21
04:24
04:27
04:30
04:33
04:36
04:39
04:42
04:45
04:48
04:51
04:54
04:57
05:00
05:03
05:06
05:09
05:12
05:15
05:18
05:21
05:24
05:27
05:30
05:33
05:36
05:39
05:42
05:45
05:48
05:51
05:54
05:57
06:00

Figure S3. 1D and 2D gel analysis of DSBs and COs from LatB meiotic time course

(B) 2D gel analysis of SEIs and dHJs from LatB meiotic time course. (C) Crossovers (CO-1) and non-crossovers (NCO-1) analysis with *HIS4LEU2* tester construct.

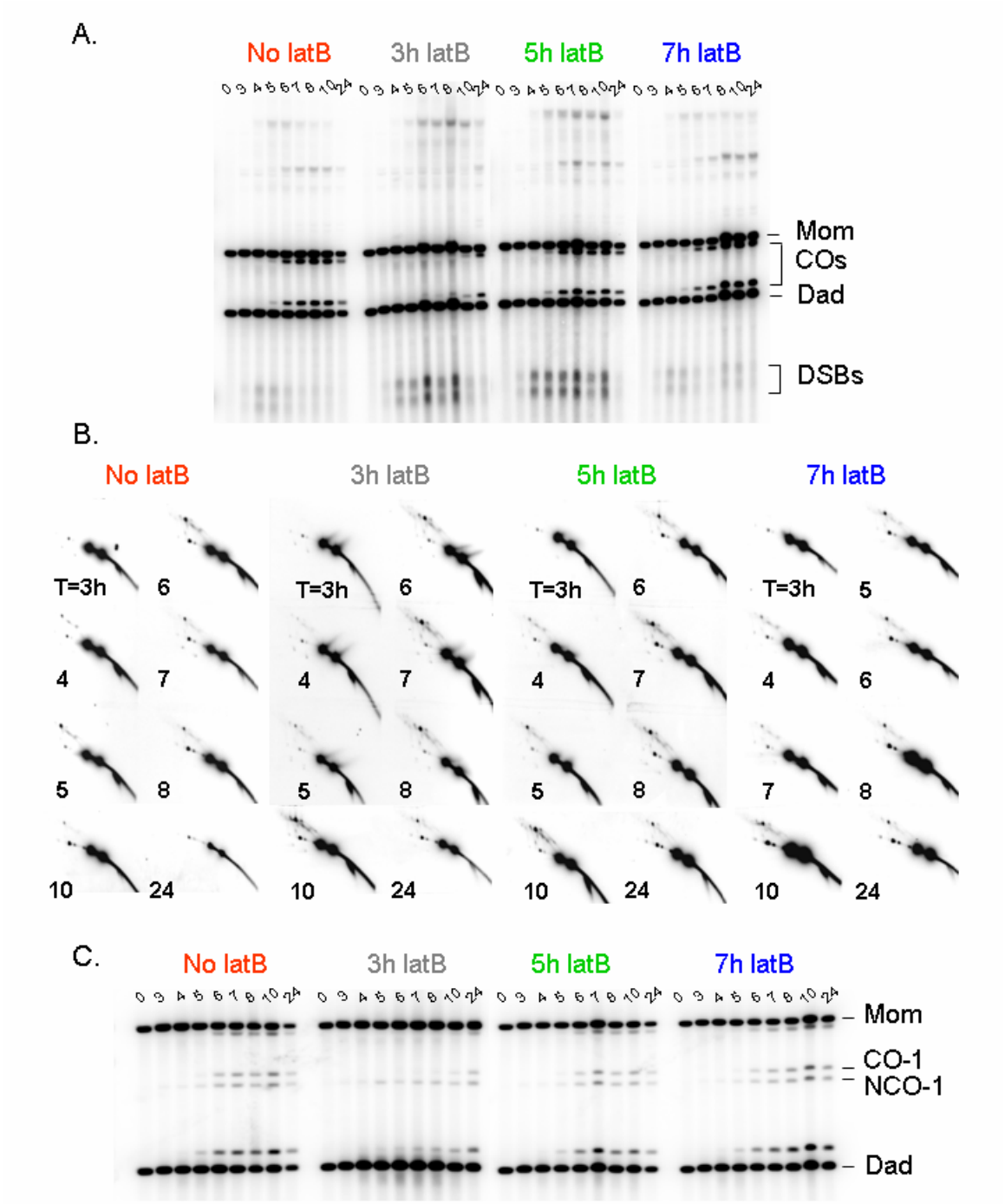

Figure S4. Zygotene/pachytene chromatin status (A) Changes in overall chromosome state in budding yeast. Squashed DAPI-stained chromosomes of the indicated morphologies occur sequentially through meiosis in correlation with known stages of recombination and SC formation as determined by parallel analysis of the same time course. (B) Chromatin and SC morphologies of budding yeast chromosomes characteristic of zygotene/pachytene transition (left) and at mid-pachytene (right) as visualized by spreading, silver-staining and EM visualization from the same experiment described in (A). (C) Sordaria chromosomes are floppier at mid-zygotene and become stiffer into mid-pachytene with stages defined both by extent of SC formation and nucleus size (from Kleckner et al., 2004; Copyright (2004) National Academy of Sciences, U.S.A.).